

Extension of Process Limits in High-Strength Aluminum Forming by Local Contact Heating


Erik Sellner,* Yikai Xu, and Peter Groche

The aluminum alloy EN AW-7075 T6 is used in the automotive sector for its favorable strength-to-weight ratio. However, the limited cold formability is currently addressed by energy- and time-consuming temperature-assisted processes. In order to limit the effort to critical forming areas only, the state-of-the-art shows promising results for increasing the blank temperature in the range of warm forming. The design of new processes in an industrial context requires appropriate numerical simulation with inherent complexity due to time- and temperature-dependent effects. Herein, the potential of a newly developed tool setup and process chain with integrated local contact heating of the EN AW-7075 T6 blank is investigated on the basis of a curved hat profile. A thermomechanically coupled FE model of the process is developed and validated. The influence of the local heating layout is analyzed in experimental forming tests and a corresponding process window is derived. The influence of local heating on the occurring failure mechanisms is discussed based on simulation results. The equivalent plastic strain evolution is successfully used to evaluate the local heating dependent failure behavior. A significant increase in the overall formability of the part is achieved by the proposed process chain.

1. Introduction

Increasingly stringent regulations on the sustainability of cars and trucks are a growing challenge for manufacturers.^[1] At the same time, increasing demands for comfort and safety must be met. Given the current electrification in the automotive sector, low vehicle weight is of particular importance. One solution is lightweight design, for which high-strength aluminum alloys such as EN AW-7075 are particularly suitable due to their high strength-to-density ratio.^[2] These are used for body-in-white and crash-relevant components in particular.^[3] They are most commonly delivered in the high-strength T6 condition due to its stability over time. However, these alloys have not yet been

E. Sellner, Y. Xu, P. Groche
Institute for Production Engineering and Forming Machines
Technical University of Darmstadt
Otto-Berndt-Straße 2, 64287 Darmstadt, Germany
E-mail: sellner@ptu.tu-darmstadt.de

 The ORCID identification number(s) for the author(s) of this article can be found under <https://doi.org/10.1002/adem.202201940>.

© 2023 The Authors. Advanced Engineering Materials published by Wiley-VCH GmbH. This is an open access article under the terms of the Creative Commons Attribution-NonCommercial-NoDerivs License, which permits use and distribution in any medium, provided the original work is properly cited, the use is non-commercial and no modifications or adaptations are made.

DOI: 10.1002/adem.202201940

widely used due to their low formability at room temperature.^[4] It is well known that forming of aluminum at elevated temperatures allows for increased formability.^[5] As a result, several temperature-assisted forming processes, such as hot forming, warm forming, and W-Temper forming, have been investigated in the past and are being used in the industry. A comprehensive review of current developments can be found in Zheng et al.^[6]

During the hot forming and die quenching process, the EN AW-7075 blank is undergoing solution annealing (SA) at 460–480 °C. The subsequent forming and quenching of the part is done simultaneously and the necessary quenching time extends the cycle times. Artificial aging is required to achieve T6 condition again.^[7] The W-Temper condition is achieved after SA and additional quenching. The forming process takes place at room

temperature and takes advantage of a significant increase in formability for a limited time period after quenching. Both hot forming and W-Temper forming require subsequent artificial ageing by heat treatment to restore the high strength T6 condition.^[4,8] Min et al. significantly shorten the necessary artificial ageing cycles compared to conventional approaches while achieving similar high-strength properties.^[9] Both processes require energy-intensive SA of the entire blank prior to forming, regardless of the part geometry, which increases cycle times.

Alternatively, warm forming is carried out at temperatures below the recrystallization temperature.^[5] For bending of 7xxx, a temperature of 180 °C is recommended.^[10] In particular, EN AW-7075 T6 shows a significant increase in formability at temperatures between 140 and 200 °C while maintaining its initial high strength properties in the finished part.^[2,11–13] Losses in strength properties at higher temperatures can be recovered during industrial paint bake cycles.^[14]

Positive effects can be achieved by locally increased temperatures. Nonisothermal forming by heating the flange area while keeping the punch at a lower temperature increases the deep drawing capacity for aluminum forming.^[15,16] In any case, when heating large tool sections, the design is complex to ensure temperature homogeneity.^[17]

Another approach to increasing forming limits is the use of Tailored Heat Treated Blanks, where local heat treatment is used to create inhomogeneous properties for favorable material flow during forming at room temperature. It was found that softening only critical areas in the forming zone is favorable compared to

softening the entire forming zone.^[18] Design principles for the zone layout have been derived and applied to complex parts such as cross-cup and B-pillar.^[19] Local heating of the blank can be achieved by light radiation (laser), electromagnetic induction, or direct contact conduction heating. The latter allows rapid heating of large blanks compared to the other technologies.^[20] A direct comparison shows its advantage of very good reproducibility and high productivity for industrial applications.^[18] Contact heating is successfully used for local SA of 6016.^[21]

However, the very local manipulation of material properties has not yet been applied to warm forming of the high-strength aluminum alloy EN AW-7075. Therefore, the aim of this article is to investigate an efficient temperature-assisted process to increase formability and prevent failure by locally increasing the temperature of the blank in-line to warm forming condition using tool-integrated contact heating.

2. Experimental Section

2.1. Process Definition for the Application of Local Heating Units

The process route for temperature-assisted forming by local contact heating of the blank is proposed and used in this investigation, as shown in **Figure 1**. In this process, the blank heating is achieved by conductive heat transfer from active tool

components, referred to as Local Heating Units (LHUs), to specific areas of the blank. These LHUs should be integrated into the tool and heat critical areas of the blank during the press stroke to shorten cycle times and limit heat losses. This process is achieved by the depicted kinematics and characteristic operating positions of the LHU. From the initial position, the LHU contacts the blank during the closing motion and is compressed. In this second position, the blank is pressed against the blankholder by the LHU and heat is transferred from the heated cylinder for a specific period of time. Once the press reaches a set position, the LHU is retracted to be flush with the die surface. This position is maintained during the forming process. There is no significant contact pressure between the LHU and the blank due to the distanced blankholder.

2.2. Tool Design for Process- and Tool-Integrated LHU Application

In order to implement the process described in **Figure 1**, a multipurpose forming tool was designed as shown in **Figure 2a**. The lower part of the tool houses the blankholder mounted on gas springs. The punch is positioned at the tool center. The punch force is measured by two load cells type C2S (MecSense Messtechnik GmbH) positioned below the punch. The upper part of the tool consists of the die and multiple LHUs, as shown in **Figure 2b**. The LHU consists of

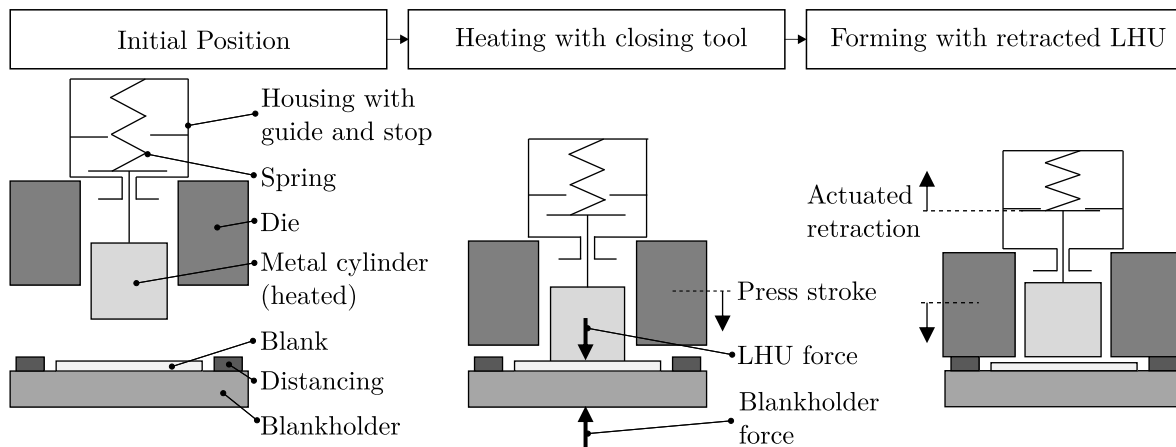


Figure 1. Schematic representation of the process of local contact heating with corresponding kinematics of the LHU in the characteristic operating positions.

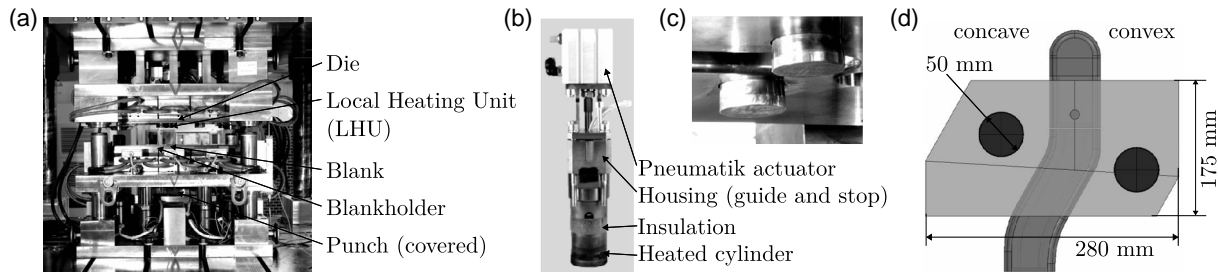


Figure 2. a) Tool setup inside the press, b) LHU components, c) installed LHUs protruding from the die surface, and d) positioning of the blank on the curved punch.

a 50 mm-diameter cylinder with electrical heating cartridges and a Type K thermocouple at 1 mm distance from the ground bottom surface. The active cylinder of each LHU can be independently set between room temperature and 450 °C using an external closed-loop controller. Temperatures above 450 °C may lead to failure of the heating cartridges in the present setup. Once the target temperature is reached, it is kept constant. The active cylinder is mounted to the guiding with insulation type K-ThermAS 800M (AGK Hochleistungswerkstoffe GmbH) in between. The housing is mounted to the die and holds the guiding, allowing for 20 mm of vertical travel. The moving part of the LHU is spring-loaded with a return force ranging from 350 N (bottom end point) to 680 N (upper end point). It is raised by the pneumatic actuator, which is triggered by an electric pushbutton at a set tool position. The LHUs are positioned in cylindrical cut-outs in the die. They protrude 20 mm from the die surface at their lower end point, as shown in Figure 2c. During forming, the die and blankholder are spaced by 1.7 mm by means of distancing cylinders. The curved punch has a concave and convex radius in the style of the 2008 Numisheet benchmark study and corresponding blank dimensions, as shown in Figure 2d.^[22] The outer edges of the blank are milled to avoid edge cracking. Due to the tool and blank setup, the forming operation corresponds to a bending with curved edges and spaced blankholder application.^[23] The LHUs are positioned in the flange area of the blank in the concave and convex radii, respectively, as shown in Figure 2d.

Table 1. Test parameters LHU applied in bending with curved edges and distanced blankholder.

Parameter	Setting or value
Alloy and temper	EN AW-7075 T6
Sheet thickness	1.5 mm
Lubricant	MKU Putrol NW V 1933-30 N-1
Punch radius/die radius	5 mm/6.5 mm
Punch wall angle	3°
Punch convex/concave radius	40 mm/50 mm
Blankholder distancing	1.7 mm
Blankholder stroke/forming stroke	95 mm/75 mm
Average forming speed	100 mm s
LHU heating configurations	Concave/convex/concave and convex
LHU temperatures	Room temperature, 200, 300, 350, 400, and 450 °C

The blank is positioned by a pin mounted on the punch while it is manually aligned with a stop bracket. The multipurpose forming tool is mounted in a servo-electric press SWP 2500 (synchropress GmbH), which allows positions to be held for specified periods of time.

2.3. Forming Trials

The test parameters used in the experimental investigation are listed in Table 1. Aluminum alloy EN AW-7075 was used in its as-delivered condition T6 with a thickness of 1.5 mm. All active forming tools in contact with the blank are made of hot work tool steel Unimax (Uddeholm, voestalpine High Performance Metals Deutschland GmbH) at 57 ± 1 HRC with polished die and punch radii. The forming tool and blanks were lubricated with mineral oil Putrol NW V 1933-30 N-1 (MKU-Chemie GmbH) and applied manually by brush. Once the LHU reaches the set temperature, the blank is positioned by a pin mounted on the punch and manually aligned with a stop bracket.

The four-stage forming process follows the press stroke shown in Figure 3a. First, the press is closed and the LHUs are compressed by 10 mm after blank contact. The tool is then held at a constant position for 2 s. The press then continues closing and the LHUs are retracted before distancing comes into contact. Finally, the blankholder is displaced for 95 mm where forming takes place for the last 75 mm. The press movement is composed of sinusoidal function segments.

The punch force and blankholder displacement are measured during each test. The time of failure due to cracking, splitting, or tearing is determined from the force signal. The corresponding drawing depth is calculated from the blankholder position at which the failure occurred, as shown in Figure 3b.

To validate the simulation, selected samples are cleaned after forming and the surface is digitized using the 3D optical measurement system ATOS (Carl Zeiss GOM Metrology GmbH). The simulation is then fitted to the experimental surface in the punch radii using a Gaussian best-fit method.

2.4. FE Modeling

This section describes the FE model used to simulate the process described in the previous sections. It is represented in a 3D thermomechanical model in Abaqus 6.14-1, as shown in Figure 4a. The simulation of heat transfer and forming is modeled using an explicit solver. The subsequent springback is simulated using an

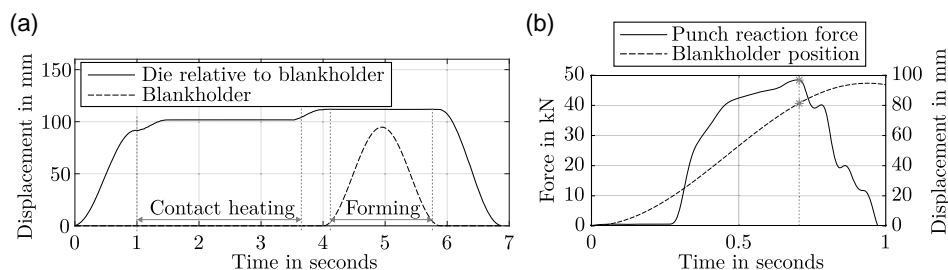


Figure 3. a) Measured die displacement relative to the blankholder and blankholder displacement for a single trial; b) example determination of drawing depth at failure.

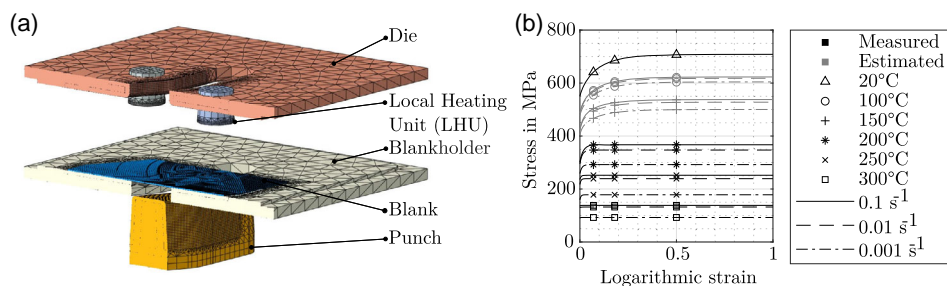


Figure 4. a) Sectional view of the FE model and b) flow curves for EN AW-7075 T6 at different temperatures and strain rates.

implicit solver with a damping coefficient of 0.02. The die displacement is approximated with sinusoidal function segments following the experimental press stroke. The test parameters used in the numerical investigation are shown in **Table 2**.

The blank is modeled elastoplastically using von Mises plasticity with isotropic hardening. It is specified by temperature- and strain rate-dependent flow curves shown in Figure 4b. The curve at 20 °C is obtained from uniaxial tensile tests performed by the authors. The curves at 200, 250 and 300 °C are based on the results of uniaxial tensile tests on the same batch of material.^[24] They are determined for different strain rates to account for the dependence shown by Sotirov et al.^[25] The Hockett–Sherby approach is used to approximate the flow curves.^[26] Flow curves for 100 °C and 150 °C at 25% and 50% stress are added by the authors between the 20 and 200 °C flow curves. These curves are in good agreement with the literature and take into account the nonlinear change in plastic properties at this temperature range.^[12,27] All other components are modeled as rigid and discretized to account for heat conduction. Each component is set to an initial temperature using homogeneous predefined fields. Normal contact behavior between tool, LHUs, and blank is modeled with an exponential contact behavior. Tangential contact behavior is modeled with a constant coefficient of friction of 0.01 according to Schell et al.^[28]

Table 2. Parameters for the thermomechanical FE heating and forming simulation.

Parameter	Setting or value
Specific heat (30–500 °C)	Unimax: 460–656 J kg ⁻¹ K ⁻¹ ^[34,35] 7075-T6: 863–1102 J kg ⁻¹ K ⁻¹ ^[36]
Thermal conductivity (20–500 °C)	Unimax: 27–29 W m ⁻¹ K ⁻¹ ^[34] 7075-T6: 121–158 W m ⁻¹ K ⁻¹ ^[36]
Normal contact behavior	Surface-to-surface exponential soft contact: $p(5 \mu\text{m}) = 0 \text{ MPa}$; $p(0 \mu\text{m}) = 3 \text{ MPa}$
Tangential contact behavior	Coulomb friction coefficient = 0.01 ^[28]
Elements in blank contact	Element type C3D8T Blank maximum size: $2 \times 2 \times 0.5 \text{ mm}^3$ ($l \times w \times h$) Tool average size: $2 \times 2 \times 2 \text{ mm}^3$ ($l \times w \times h$) Refined punch and die radii: eight elements
IHTC-function parameters ^[30]	Gap: $\text{IHTC}(p = 0 \text{ MPa}, c = 0 \text{ mm}) = 0.7 \text{ kW m}^{-2} \text{ K}^{-1}$ Pressure: $\text{IHTC}_{\text{max}} = 9 \text{ kW m}^{-2} \text{ K}^{-1}$; $p_{50} = 0.5 \text{ MPa}$

Investigations with the same tool, aluminum alloy, and lubricant at varying temperatures show no significant changes.^[29] Heat transfer between tool and blank and LHUs and blank is modeled, using the gap and pressure-dependent interfacial heat transfer coefficient (IHTC) according to the approach presented by Sellner et al.^[30] The IHTC in the gap and pressure-free condition is consistent with the results of Liu et al.^[31] The simulation time is reduced by using a mass scaling factor of 100 for forming and 10 000 for others. It is found that the mass scaling has no significant effect on the forming results. A finer mesh is applied to the areas of the tool in contact with the blank. The element sizes are determined by convergence analysis. From the simulations, stress triaxiality and equivalent plastic strain (PEEQ) are analyzed among others.^[32]

2.5. Hypothesis and Scientific Question

The potential of the LHU is methodically evaluated in the subsequent sections using the following assumption and questions.

Thesis 1: Localized blank heating increases the overall formability of the entire component.

Thesis 2: Process capability can be assessed based on critical plastic deformation.

Question: What principles can be derived for the process design in terms of LHU layout and their temperature?

3. Results and Discussion

Section 3.1 shows geometrical and punch reaction force results to validate the FE model. The simulation results in Section 3.2 show the relation between the stress state in the blank during forming and the temperature distribution due to local heating. Section 3.3 presents the forming test with local heating and discusses them with further simulation results.

3.1. Validation of the FE Model

Validation of the FE model is carried out using OK parts for selected combinations of the LHU application. The surface offset of the experimental geometry is plotted against the simulated geometry shown in **Figure 5a**. In general, the area at the punch shows deviations of less than 1 mm. It increases toward the wall and flange areas due to the amplifying effect of the springback angle with increasing wall height. The positive distance

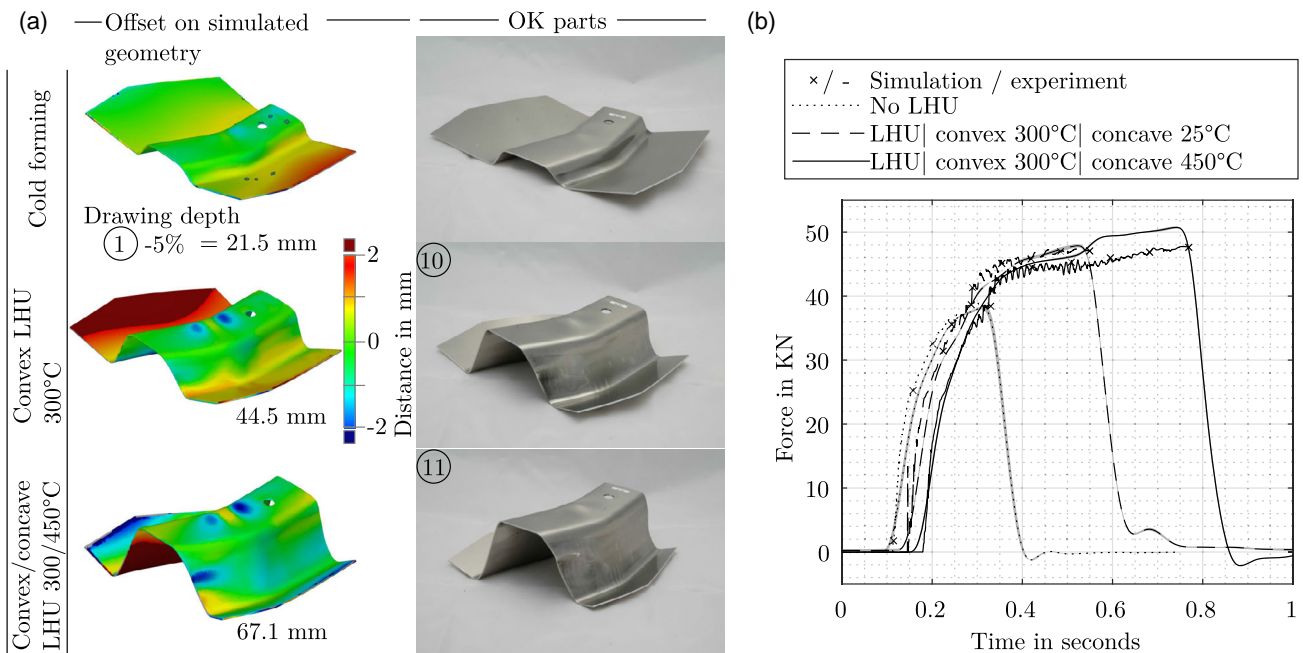


Figure 5. a) Validation of numerical simulation by geometrical offset and b) punch reaction force for OK trials using different LHU heating settings (sample number referring to Figure 9 and 10).

represents an underestimation of the springback in the simulation with the experimental surface above the simulated surface.

The simulated punch reaction force during forming is compared with the measured force in Figure 5b. It is underestimated by up to 4 kN for both LHUs applied after 0.6 s. At this point, the heated concave flange area is drawn into the die radius. It can be assumed that increased friction occurs at the die radius in the experiment, which is not accounted for in the FE model. In summary, the FE model is in good agreement with both the part geometry and the forming forces.

3.2. Simulation Results for the Application of the LHU

Figure 6 presents the effect of the LHU application in the concave and convex areas of the blank for varying temperatures

and drawing depth. The simulation results show a concentration of compressive stress in the convex flange area and tensile stress in the concave flange area as shown in Figure 6a. These areas overlap with the areas of increased temperature in the blank when LHUs are applied. As the drawing depth increases, the qualitative stress distribution remains in a constant position relative to the tool while the heated blank area is transferred to the wall section of the hat profile.

The simulated blank temperature at the center of the LHU is shown in Figure 6b. In addition to the constant holding time, additional heating occurs for 0.7 s due to the delay in compression and retraction of the LHU. Temperature saturation is achieved within the set heating time. Maximum temperatures reach 50% of the initial LHU temperature. The reduction in blank temperature prior to forming is limited to 25 °C.

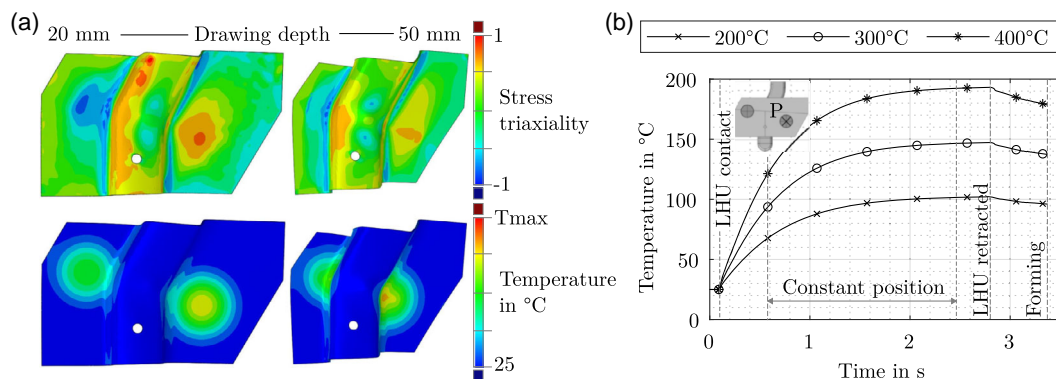


Figure 6. a) Distribution of stress triaxiality and temperature of the blank after LHU application for 20 and 50 mm of drawing depth (convex LHU: 300 °C, concave LHU: 400 °C); b) simulated temperature increase of the blank at the LHU center point P for varying symmetric LHU temperatures.

Increasing the forming speed can reduce these losses before and during forming. However, the material is very sensitive to strain rate at warm forming temperatures, which could result in a reduced formability. Significant changes in the plastic properties of the blank can be expected in the temperature range reached at the selected forming speed.

3.3. Forming Trials with LHU Application

This section presents the experimental results on the dependency of drawing depth for concave (Section 3.3.1), convex (Section 3.3.2), and double-sided (Section 3.3.3) LHU applications. The corresponding failure patterns are discussed using simulation results.

In general, the forming tests show no evidence of adhesion or surface damage to the blanks. This is due to the avoidance of contact normal pressure during the relative movement between the LHUs and the blank, and the distancing of the tool. In addition, the localized short-term heat transfer limits the area susceptible to increased wear.

3.3.1. Concave Heating

The drawing depths achieved at the time of failure for the forming test without LHU application and with increasing temperature of the concave LHU are shown in **Figure 7**. The convex LHU is permanently set at room temperature. Without LHU support, the drawing depth shows a large scatter between 24 and 61 mm. Distinct failure patterns can be identified. Early failure occurs from 17 to 27 mm (sample 1). The typical failure pattern is a fracture in the die radius area of the unheated convex side. This failure mode is similar to the tearing of sidewalls at the base of deep drawn cups. It occurs as a result of the initial stretch forming condition, which causes increased thinning of the blank. As the wall transfers the load from the forming area to the punch,

critical tensile stresses in the order of the tensile strength can lead to failure. Tearing usually occurs at the edge with the smaller radius.^[23] In this study, the elastic deformation of the blank results in a larger bending radius above the punch than over the die, where the blank is constrained by the distanced blankholder. The concave LHU, located on the opposite side of the point of failure, does not transfer temperature into the critical area. As a result, it has no significant effect on this specific failure mode.

Cold formed samples at higher drawing depths show initial tearing at the blank edge of the concave wall extending to the punch edge area (sample 2). The simulation results show the maximum value of PEEQ near the wall edge. This value is significantly reduced at the equivalent drawing depth when the concave LHU is applied (simulation 3'). As a result, the failure pattern no longer occurs. A critical value of PEEQ can be assumed due to the limited plastic deformation of the material before failure occurs. This will be discussed further in Section 3.4.

A third group of specimens is found at failure levels between 53 and 62 mm when concave LHU is applied. The corresponding failure pattern is a fracture in the wall section of the unheated convex side (sample 3). The samples show wrinkling of the blank at the corresponding local area of increased PEEQ in the simulation. Failure in this area may be caused by the change from compressive to tensile stress state at the transition from the forming zone in the flange to the wall. The unfavorable stress state then results in a reduced critical value of PEEQ.

Consequently, applying the LHU to the concave side does not prevent failure at low drawing depths. The critical case for this configuration is identified as the unheated convex side of the profile due to tearing at the die radius after stretch forming.

3.3.2. Convex Heating

In **Figure 8**, the attained drawing depth at the time of failure is shown for cold forming and increasing convex LHU

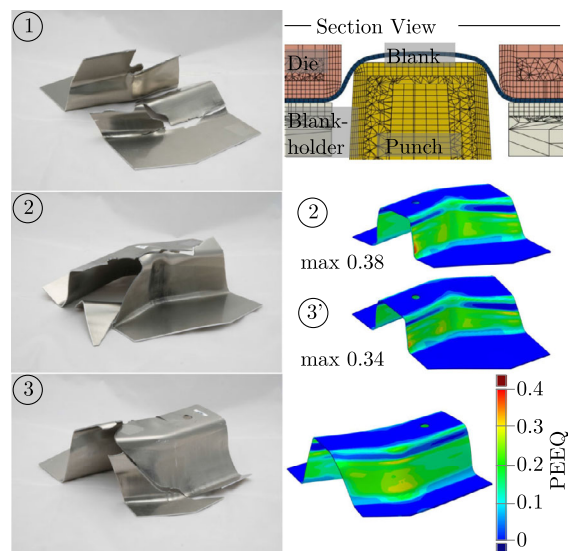
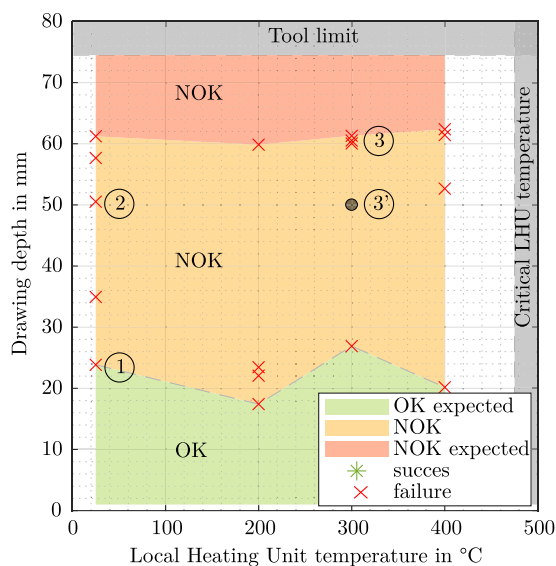


Figure 7. Process limits in terms of drawing depth for different concave LHU temperatures with typical fracture distributions and corresponding simulation results.

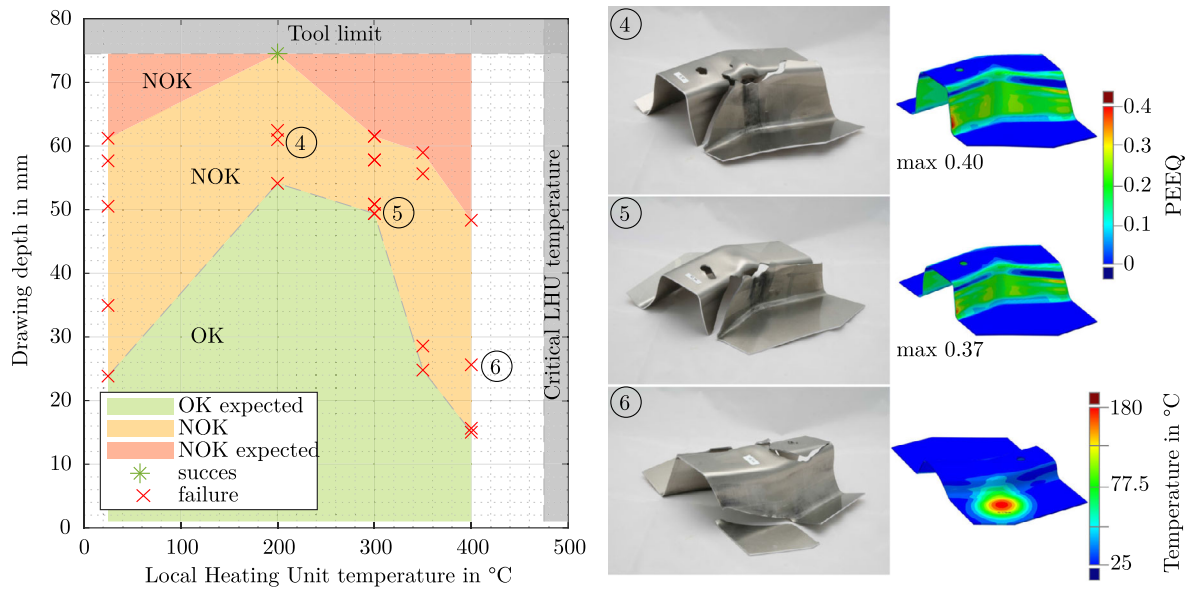


Figure 8. Process limits in terms of drawing depth for different convex LHU temperatures with typical fracture distributions and corresponding simulation results.

temperature. The concave LHU is permanently set at room temperature. The results for the unheated test are discussed in Section 3.3.1.

The drawing depth increases to 54 and 49 mm at LHU temperatures of 200 and 300 °C, respectively. The specimens show a characteristic failure pattern with initial tearing at the blank edge of the concave wall extending to the punch edge area (sample 4 and 5). The pattern is similar to sample 2 in Figure 7 for cold forming at 50 mm drawing depth. The maximum value of PEEQ is similar and especially higher for sample 5 compared to the simulation of concave LHU heating in Figure 7 at the drawing depth 3'. Consequently, this failure is caused by limited plastic deformation of the material without LHU application. Again, a critical value of PEEQ can be assumed and will be discussed further in Section 3.3.3.

The local temperature increase in the convex primary forming zone reduces the yield stress, allowing more plastic deformation to take place, thereby reducing the stress transferred in the critical blank section at the die radius. As a result, the critical failure mode in the thinned blank section after stretch forming identified for sample 1 in Section 3.3.1 is avoided for convex LHU applications at 200 and 300 °C.

At higher LHU temperatures of 350 and 400 °C, failure occurs at lower drawing depths. The corresponding specimens show initial tearing at the blank edge of the convex side as can be seen for sample 6. The simulation at the corresponding drawing depth shows that the blank area of increased temperature and reduced yield stress is drawn into the die radius and wall section. Failure is likely due to the reduced load-carrying capacity of this heated blank area, which increases stress in the surrounding areas, leading to critical stress levels in the die radius adjacent to the heated area.

It can be concluded that the use of the convex LHU increases formability by preventing early failure at the convex die edge. Temperatures above 300 °C reduce the drawing depth and lead

to failure characteristics caused by excessive local softening of the material. The critical failure zone of this configuration at optimum LHU temperatures is on the unheated concave side at greater drawing depths due to higher levels of plastic deformation in the heated area. Therefore, a convex LHU temperature of 300 °C is used for double-sided heating, as presented in Section 3.3.3.

3.3.3. Double-Sided Heating

The use of a single LHU on the concave side (Section 3.3.1) or convex side (Section 3.3.2) of the hat profile results in a characteristic distribution of the failure patterns at specific drawing depths. This allows the critical failure zone to be located on the opposite side to where the LHU is applied. As shown in Figure 6a, the areas of increased temperature do not overlap when heating is combined on both the concave and convex sides due to the distance, the localized heat transfer from the LHUs, and the short time to forming. It can therefore be assumed that the positive effects of each individual LHU can be superimposed to further increase formability. The convex LHU application prevents the more critical failure at the convex die radius (see Section 3.3.2). It is therefore set at 300 °C and the concave LHU temperature is varied for the following tests.

The drawing depth achieved at the time of failure is shown in **Figure 9**. It increases with increasing concave LHU temperature from 49 to 59 mm at 400 °C. The characteristic failure pattern with initial tearing at the blank edge of the concave wall extending to the punch edge area of samples 7 and 8 is similar to samples 4 and 5 in Figure 8. The corresponding simulation results show the critical area of high plastic deformation.

Individual samples show no failure when concave heating is applied. At a concave LHU temperature of 450 °C, no failure can be detected at the tool drawing limit of 75 mm (sample 9). The

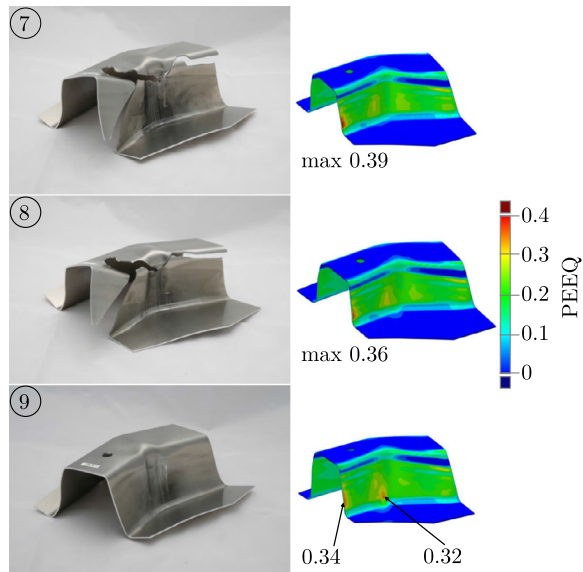
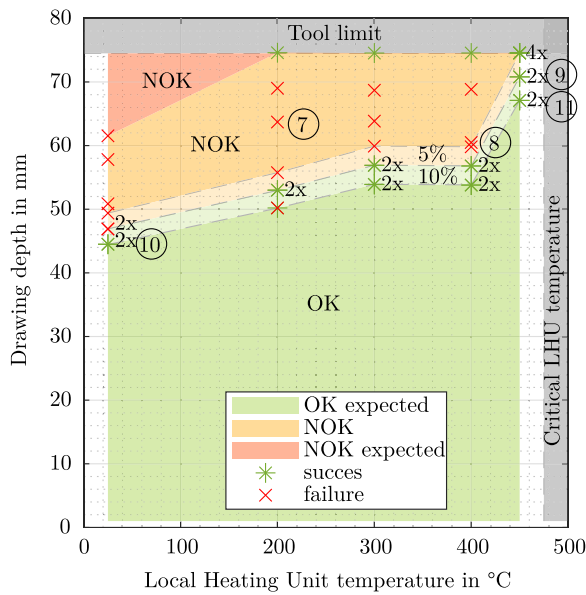


Figure 9. Process limits in terms of drawing depth for convex LHU at 300 °C and various concave LHU temperatures with 5% and 10% safety limits (dashed lines), typical fracture distribution, and corresponding simulation results. The number of test is given for the same drawing depth.

simulated PEEQ value in the critical wall area is drastically reduced compared to lower concave LHU temperatures. The expected NOK limit is successfully validated by additional forming trials at 5% and 10% reduced drawing depth compared to the earliest failed sample as shown in Figure 3.1.

It can be concluded that the use of local heating in the convex and concave blank areas increases the formability of the overall part by preventing early failure at the convex die edge and later failure at the concave wall, respectively. This confirms Thesis 1 from Section 2.5.

3.4. PEEQ as a Process Design Criteria

The failure patterns examined in Section 3.3.3 in particular do not show significant thinning due to forming with a spaced blankholder. As a result, the failure criterion of forming limit diagram (FLD) based on failure due to local necking is not suitable to characterize changes in formability. However, there are a number of ductile damage models that are primarily dependent on the plastic strain and stress triaxiality.^[33] The failure pattern and location are similar in the tests with double-sided LHU application presented in Figure 9; thus, a comparable stress triaxiality condition can be assumed. The plastic strain critical for failure can therefore be considered in a simplified manner using PEEQ. By analyzing the PEEQ value of the area critical for failure of the component, the influence of local heating on the failure limit is investigated in order to answer the question of Section 2.5.

For closer examination, the simulated PEEQ evolution along the drawing depth for the node with maximum PEEQ at failure or at the end of the test of each sample from Figure 9 is shown in Figure 10. It can be seen that the maximum PEEQ value for these critical nodes (highest overall PEEQ in the part) decreases at similar drawing depth as the concave LHU temperature increases. The lowest value of 0.347 is obtained at the highest temperature

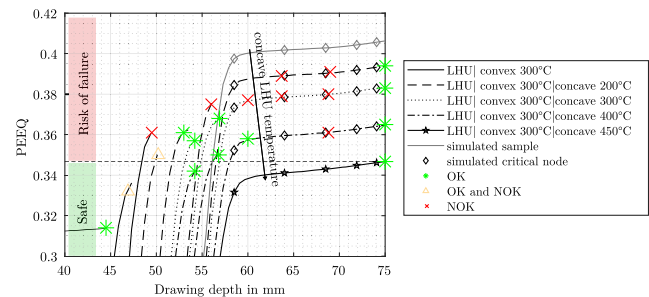


Figure 10. Simulated development of equivalent plastic strain PEEQ of the critical node at failure or trial end for varying LHU temperatures (tests similar to Figure 9).

of 450 °C. Tests with similar or lower PEEQ values can be considered safe as four OK tests were observed for this setting. Tests with higher PEEQ values, typically for lower LHU temperatures, have an increasing risk of failure.

As can be seen from the diagram, concave heating is an effective method of moving the critical PEEQ in this area of the sheet towards safe values at higher drawing depths. This is due to a change in the distribution of plastic deformation. As the temperature in the concave forming zone increases locally, the plastic deformation in the heat-affected zone also increases. This allows for the resulting deformation in the adjacent unheated zones to be reduced while maintaining the overall geometry of the part. Both can be seen in the PEEQ distribution of sample 9 in Figure 9.

4. Conclusion and Outlook

In this article, a method for a tool- and process-integrated local contact heating of EN AW-7075 T6 aluminum blanks is proposed

and implemented in a tool design. A thermomechanically coupled FE model is developed and validated with good overall agreement, allowing the identification of critical blank areas and failure mechanisms. The simulated maximum temperatures and short heat influence times of less than 3 s show promising results in terms of maintaining strength properties.^[12]

LHU application in the convex forming zone is found to prevent early failure due to tearing in thinned out blank sections. The application of LHU in the concave forming zone further increases the drawing depth by reducing critical plastic deformation in the unheated adjacent area. These effects are superimposable. The results of experimental tests show effective failure prevention with LHU application and an increase in drawing depth of 211 % compared to forming at room temperature, confirming Thesis 1 formulated in Section 2.5.

Thesis 2 can also be confirmed, as the process capability can be assessed by analyzing critical PEEQ concentrations and their change due to LHU application. However, the results have limited applicability to the part geometry and LHU layout presented in this article. The FE model can be applied to flexible process design of further geometries by using a ductile failure criterion suitable for the aluminum alloy EN AW-7075.

To answer the scientific question formulated in Section 2.5, the results presented in this article allow the definition of design principles for LHU layout and their temperature setting: 1) Local blank heating indirectly avoids areas of critical deformation by facilitating the plastic deformation in surrounding areas and influencing the material flow. 2) LHUs should be placed in areas of stress concentration in the primary forming zone to facilitate local plastification. 3) A minimum LHU temperature is required to achieve warm forming conditions in localized blank areas, depending on the heat losses. Raising the LHU temperature above a critical limit can cause in premature failure by creating local weak spots.

The results indicate a promising way to efficiently increase formability of complex high-strength aluminum parts by targeted local contact heating of the blank.

Acknowledgements

The analyses in this article were carried out as part of the dual doctorate program of the "ProsiAl dual" project in cooperation with Hörmann Automotive Gustavsburg GmbH. This project (HA project no. 1269/21-170) was financed with funds of LOEWE—Landes-Offensive zur Entwicklung Wissenschaftlich-ökonomischer Exzellenz, Förderlinie 3: KMU-Verbundvorhaben (State Offensive for the Development of Scientific and Economic Excellence).

Open Access funding enabled and organized by Projekt DEAL.

Conflict of Interest

The authors declare no conflict of interest.

Data Availability Statement

Research data are not shared.

Keywords

high-strength aluminum, local contact heating, thermomechanically coupled simulation, warm forming

Received: December 31, 2022

Revised: April 17, 2023

Published online: June 14, 2023

- [1] Das Europäische Parlament und der Rat der Europäischen Union VERORDNUNG (EU) 2019/631 DES EUROPÄISCHEN PARLAMENTS UND DES RATES zur Festsetzung von CO₂-Emissionsnormen für neue Personenkraftwagen und für neue leichte Nutzfahrzeuge und zur Aufhebung der Verordnungen (EG) Nr. 443/2009 und (EU) Nr. 510/2011: VO (EU) Nr. 631/2019., <https://eur-lex.europa.eu/legal-content/DE/TXT/HTML/?uri=CELEX:32019R0631&from=DE> (accessed: December 2022).
- [2] D. Uffelmann, *ATZextra* **2010**, 15, 22.
- [3] European Aluminium Association Aluminium Automotive Manual: Applications – Car Body – Body Components, **2013**, <https://european-aluminium.eu/blog/aluminium-automotive-manual/>, (accessed: February, 2019).
- [4] J. Mendiguren, E. Argandona, L. Galdos, *IOP Conf. Ser.: Mater. Sci. Eng.* **2016**, 159, 012026.
- [5] R. Neugebauer, T. Altan, M. Geiger, M. Kleiner, A. Sterzing, *CIRP Ann.* **2006**, 55, 793.
- [6] K. Zheng, D. Politis, L. Wang, J. Lin, *Int. J. Lightweight Mater. Manuf.* **2018**, 1, 55.
- [7] K. Zheng, Y. Li, S. Yang, K. Fu, J. Zheng, Z. He, S. Yuan, *J. Manuf. Mater. Process.* **2020**, 4, 76.
- [8] N. Rigas, H. Schmid, M. Merklein, *CIRP J. Manuf. Sci. Technol.* **2022**, 37, 11.
- [9] J. Min, F. Xie, Y. Liu, Z. Hou, J. Lu, J. Lin, *IOP Conf. Ser. Mater. Sci. Eng.* **2021**, 1157, 012048.
- [10] Gesamtverband der Aluminiumindustrie, Wärmebehandlung von Aluminium-Legierungen. *GDA*, **2007**.
- [11] P. Schulz, J. Berneder, D. Uffelmann, C. Zelger, C. Melzer, *Mater. Sci. Forum* **2011**, 690, 451.
- [12] H. Wang, Y. Luo, P. Freidman, M. Chen, L. Gao, *Trans. Nonferrous Metals Soc. China* **2012**, 22, 1.
- [13] B. Behrens, H. Vogt, M. Jalanesh, C. Bonk, H. Maier, S. Behrens, *Warmumformung von 7xxx-Aluminiumlegierungen*, Europäische Forschungsgesellschaft für Blechverarbeitung e.V., Hannover **2018**.
- [14] T. Ivanoff, E. Taleff, L. Hector, *Light Metals* **2015**, 77, 223.
- [15] P. Groche, R. Huber, J. Dörr, D. Schmoeckel, *CIRP Ann.* **2002**, 51, 215.
- [16] D. Li, A. Ghosh, *J. Mater. Process. Technol.* **2004**, 145, 281.
- [17] N. Harrison, P. Friedman, J. Pan, *J. Manuf. Process.* **2015**, 20, 356.
- [18] M. Geiger, M. Merklein, U. Vogt, *Prod. Eng.* **2009**, 3, 401.
- [19] U. Vogt, Dissertation, Univ. Erlangen, Nürnberg **2009**.
- [20] J. Raseira, K. Daun, C. Shi, M. D'Souza, *Appl. Therm. Eng.* **2016**, 98, 1165.
- [21] M. Machhammer, C. Sommitsch, *IOP Conf. Ser. Mater. Sci. Eng.* **2016**, 159, 012001.
- [22] K. Roll, K. Wiegand, P. Hora, *Proc. of the 7th Int. Conf. and Workshop on Numerical Simulation of 3d Sheet Metal Forming Processes*, Interlaken, Switzerland **2008**, pp. 45–51.
- [23] A. Birkert, S. Haage, M. Straub, in *Umformtechnische Herstellung Komplexer Karosserieteile: Auslegung Von Ziehanlagen*. Springer Berlin Heidelberg, Berlin, Heidelberg **2013**.
- [24] S. Sajadifar, E. Scharif, U. Weidig, K. Steinhoff, T. Niendorf, *Metals* **2020**, 10, 884.

- [25] N. Sotirov, P. Simon, T. Waltenberger, D. Uffelmann, C. Melzer, in *Proc. 12th Int. Conf. On Aluminium Alloys*, The Japan Institute of Light Metals, Yokohama, Japan **2010**, pp. 1237–1242.
- [26] J. Hockett, O. Sherby, *J. Mech. Phys. Solids* **1975**, *23*, 87.
- [27] M. Jäckel, S. Maul, C. Kraus, W. Drossel, *J. Phys. Conf. Ser.* **2018**, *1063*, 012074.
- [28] L. Schell, E. Sellner, M. Massold, P. Groche, *Adv. Eng. Mater.* **2023**, <https://doi.org/10.1002/adem.202201900>.
- [29] L. Schell, M. Emele, A. Holzbeck, P. Groche, *Tribol. Int.* **2022**, *168*, 107449.
- [30] E. Sellner, A. Khatib, A. Ambaye, P. Groche, *Wt Werkstattstechnik Online* **2021**, *111*, 665.
- [31] X. Liu, K. Ji, O. Fakir, H. Fang, M. Gharbi, L. Wang, *J. Mater. Process. Technol.* **2007**, 158.
- [32] Dassault Systèmes Abaqus 6.14 Online Documentation. <http://wufengyun.com/v6.14/books/usb/default.htm?startat=pt05ch22s02abm03.html>, (accessed: October, 2022).
- [33] K. Komori, *Ductile Fracture in Metal Forming: Modelling and Simulation*, Academic Press Inc, London, UK **2020**.
- [34] Voestalpine High Performance Metals Deutschland GmbH, Materialdaten_Unimax. E-Mail 22.01.2021.
- [35] UDDEHOLMS AB UDDEHOLM UNIMAX: Classified according to EU Directive 1999/45/EC. https://www.uddeholm.com/app/uploads/sites/40/2017/11/unimax-eng_p_1509_e6.pdf, (accessed: October 2022).
- [36] Z. Guo, H. Zhu, S. Cui, Y. Wang, *Trans. China Weld. Inst.* **2015**, *36*, 92.